

2016

Development Of A Luminescent Polymer Sensor Array For The Discrimination Of Carboxylates And Further Improvements In A Solvent Programmable Polymer

William J. Richardson
University of South Carolina

Follow this and additional works at: <https://scholarcommons.sc.edu/etd>

 Part of the [Chemistry Commons](#)

Recommended Citation

Richardson, W. J.(2016). *Development Of A Luminescent Polymer Sensor Array For The Discrimination Of Carboxylates And Further Improvements In A Solvent Programmable Polymer*. (Master's thesis). Retrieved from <https://scholarcommons.sc.edu/etd/3871>

This Open Access Thesis is brought to you by Scholar Commons. It has been accepted for inclusion in Theses and Dissertations by an authorized administrator of Scholar Commons. For more information, please contact digres@mailbox.sc.edu.

DEVELOPMENT OF A LUMINESCENT POLYMER SENSOR ARRAY FOR THE
DISCRIMINATION OF CARBOXYLATES AND FURTHER IMPROVEMENTS IN A
SOLVENT PROGRAMMABLE POLYMER

by

William J. Richardson

Bachelor of Science
Colorado State University, 2012

Submitted in Partial Fulfillment of the Requirements

For the Degree of Master of Science in

Chemistry

College of Arts and Sciences

University of South Carolina

2016

Accepted by:

Ken D. Shimizu, Director of Thesis

Andrew B. Greytak, Reader

Paul Allen Miller, Vice Provost and Interim Dean of Graduate Studies

© Copyright by William J. Richardson, 2016
All Rights Reserved.

DEDICATION

To my mom and dad

ABSTRACT

This thesis summarizes the work performed on two stimuli responsive polymer projects. The first project used a lanthanide based luminescent polymer to create a sensor array for carboxylate analytes. Initial attempts incorporated molecular imprinting as a means to incorporate unique selectivity into the polymer by introducing acetate, benzoate, and phenylacetate as templates prior to polymerization. This process was successful at creating unique sensing elements for the array, but the polymers lacked the specific selectivity typically seen in molecularly imprinted polymers (MIPs). Instead, a ligand displacement mechanism that relied on multiple sensors with different labile anion ligands directly complexed with the europium center was utilized. This system resulted in unique response patterns with the introduction of carboxylate analytes, which were characterized using linear discriminant analysis (LDA).

The second project re-examined our group's theory about our solvent programmable polymer (SPP). Specifically, previous evidence suggested that the SPPs undergo a conformational change when heated and then cooled in a nonpolar solvent due to a dimerization between the carboxylate functional groups. To expand the utility of this unique polymer, synthetic modifications were made to the functional monomer in order to replace the ring opened metathesis polymerization (ROMP) with free radical polymerization.

TABLE OF CONTENTS

DEDICATION	iii
ABSTRACT	iv
LIST OF TABLES	vii
LIST OF FIGURES	viii
LIST OF SCHEMES	ix
 CHAPTER 1: LUMINESCENT POLYMER SENSOR ARRAY FOR SENSING CARBOXYLATES	 1
1.1 ABSTRACT	1
1.2 INTRODUCTION	1
1.3 MIP SENSOR ARRAY	4
1.4 ANION DISPLACEMENT POLYMER SENSOR ARRAY	9
1.5 EXPERIMENTAL	21
1.6 REFERENCES	24
 CHAPTER 2: SOLVENT PROGRAMMABLE POLYMER	 26
2.1 ABSTRACT	26
2.2 INTRODUCTION	27
2.3 “TURN-OFF” DIMERIZATION	28
2.4 FREE RADICAL SYNTHESIS	30
2.5 EXPERIMENTAL	33

2.6 REFERENCES	39
----------------------	----

LIST OF TABLES

Table 1.1 Analytes and anions for sensor array	11
Table 1.2 PCA variance contributions of sensors	16

LIST OF FIGURES

Figure 1.1 Comparison of old to new polymers	5
Figure 1.2 MIP and NIP emission at 616 nm	6
Figure 1.3 Luminescent response patterns of MIP array	7
Figure 1.4 LDA plots of MIP array	8
Figure 1.5 Emission vs. concentration of A1	12
Figure 1.6 Concentration titration of A1, A2, and A3	13
Figure 1.7 Emission response of anion array	14
Figure 1.8 Emission variance of anion array	15
Figure 1.9 LDA plot of anion array	17
Figure 1.10 Reusability study of polymer array	18
Figure 1.11 Correlation of F1 to change in emission.....	19
Figure 1.12 Emission response of polymer with sulfonate host molecules	20

LIST OF SCHEMES

Scheme 1.1 Eu-salen polymer synthesis and structure	3
Scheme 1.2 Anion displacement array.....	10
Scheme 1.3 Synthesis of 2-hydroxy-4-(4-vinylbenzyloxy)benzaldehyde	21
Scheme 1.4 Salen ligand synthesis	22
Scheme 2.1 Preliminary hypothesis of SPP mechanism.....	28
Scheme 2.2 Preparation of SPP	28
Scheme 2.3 Updated hypothesis of SPP mechanism	29
Scheme 2.4 Synthesis route for acrylate functional monomer	31
Scheme 2.5 New proposed route for acrylated monomer	32
Scheme 2.6 2-amino-3-methylbenzoic acid synthesis	33
Scheme 2.7 Synthesis for functional ROMP monomer	33
Scheme 2.8 Synthesis for ROMP crosslinker	34
Scheme 2.9 Synthesis of t-butyl protected monomer	35
Scheme 2.10 Oxidation of norbornene C=C bond	36
Scheme 2.11 Acrylamide coupling reaction.....	37
Scheme 2.12 Deprotection of meth acrylamide functional monomer	38

CHAPTER 1

LUMINESCENT POLYMER SENSOR ARRAY FOR SENSING CARBOXYLATES

1.1 ABSTRACT

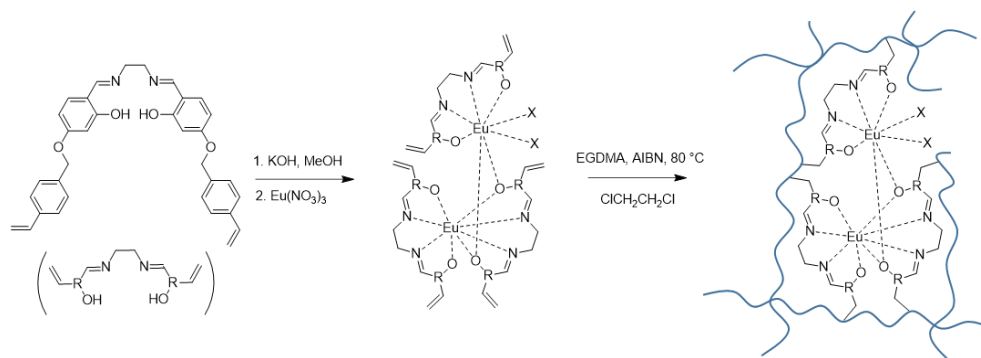
The goal of the first project was to imbue individual polymers with enough selectivity to create a luminescent sensor array capable of distinguishing structurally similar carboxylates. Initially, molecular imprinting developed for this system by Di Song and improved by Yang Xu was reproduced and analyzed using linear discriminant analysis. Despite 100% cross validation accuracy of the array, the MIPs did not show selective binding. This suggests that the array functioned as a non-specific array and the steps to achieve a MIP were excessive and unnecessary. A simpler method to create individual sensors was employed. An anion ligand exchange mechanism was designed based on the non-imprinted polymer (NIP). The exchange of anionic ligands to develop unique sensing elements proved effective and efficient. Nine carboxylic acid analytes were tested and 100% cross validation accuracy was achieved from the unique response patterns.

1.2 INTRODUCTION

A europium-based luminescent polymer sensor array was tested for applicability in distinguishing carboxylates. Luminescent and fluorescent materials are highly desirable for sensing applications because of the direct *in situ* response.^{1, 2} The two primary methods of emission-based sensing involve the analyte interacting with the sensor to produce an emission, or a static sensor that sees a modulation in its pre-existing emission based on

analyte interaction. With the second method, a change in emission intensity can either increase (turn-on) or decrease (turn-off) with the addition of an analyte. Quenching the emission, as a sensing technique, can be problematic because increasing analyte concentration decreases the signal until the signal cannot be distinguished from the baseline error. Turn-on fluorescence is preferable because it allows for a lower detection limit due to the lack of background emission. The system described in this chapter demonstrated a turn-on fluorescence with the addition of analytes.

Lanthanide fluorescence occurs at a narrow spectral bandwidth making it ideal for a variety of sensing applications. Unfortunately, the fluorescence is also very weak. However, light absorbing organic ligands can be complexed to the lanthanides to increase the emission intensity. This significant increase in intensity occurs because the excited bandgaps of the organic complex are at a higher energy level than the lanthanide. Excited electrons are therefore able to transfer into the excited energy level of the lanthanide causing a significant increase in the emission intensity of the lanthanide. The emission at 618 nm for europium has been identified as the 5D_0 to 7F_2 transition.³ Enveloping the metal ion in an organic ligand also protects the lanthanide center from solvent and self-quenching effects. A luminescent polymer based on Borovik's design shown in Scheme 1 was used as the basis for this project.⁴ This polymer system affords direct binding sites to the europium center while anchoring the complexed lanthanide into a polymer framework through free radical polymerizable vinyl groups as seen in scheme 1.1.



Scheme 1.1. Synthesis and polymerization of the Eu-salen complex designed by Borovik and co-workers with x being the binding sites for the template molecules.⁴

Carboxylic acids represent a diverse class of organic compounds that occur in nature as biological building blocks and industrially as food and pharmaceutical products.^{5,}

⁶ Due to the wide scope of uses and structural variety, sensors to detect and distinguish carboxylic acids are of significant interest. Most existing carboxylate sensor arrays are single molecule systems that require individual synthesis of sensing elements.^{7, 8, 9} The arrays presented herein are conceptually similar except that the sensing elements are not soluble and the sensing elements are based on direct interaction between the analyte and polymer-bound luminescent europium complex.

Sensor arrays have been shown as an effective strategy for differentiating similar analytes.^{10, 11, 12} Sensor arrays require a library of response data collected from the analytes against a number of individual sensing elements. Unknown analytes can then be compared against this library of patterns and classified. The intrinsic cross-reactivity of these sensors increases the dimensionality of variance in the response patterns. However, designing individual sensing elements with unique selectivity can be synthetically costly to establish. Using non-specific receptors such as polymers or polymer blends can reduce this difficulty, but with much lower selectivity. Our system seeks to establish a middle-ground with a

tunable single polymer capable of incorporating selectivity based on molecular imprinting or anion displacement.

The complexity of the response data collected from sensor arrays can be difficult to interpret without multivariate analysis. For this luminescent polymer system, the dimensional reduction technique linear discriminant analysis (LDA) was used.

1.3 MIP SENSOR ARRAY

Molecular imprinting was introduced applied to Borovik's design to attain polymers with different selectivities. Molecularly imprinted polymers (MIPs) are typically synthesized based on the interactions between template molecules and functional monomer in a pre-polymerized solution. The interactions in the pre-polymer solution are retained after polymerization, and washing out the template results in selective binding sites. This process allows for the rapid preparation of polymers with selective binding. One of the major downsides in MIP synthesis is the lack of binding site homogeneity which is caused by the low fidelity. The lack of uniform binding sites allows for a significant level of cross-reactivity that can negatively influence the MIP as a highly selective single sensor. Using several sensors as an array mitigates this problem by comparing the response patterns of analytes across the array. Sensor arrays are capable of functioning based on the interaction between different sensors and analytes regardless of the specific selectivity. Coupling this with MIPs that have a specific selectivity enables a far more useful array with minimal effort, and this approach has been used with success in the past.¹³ The typical quantification of binding to MIPs is indirect relying on UV absorption of the unbound analyte. The system discussed herein is superior to previous systems because the response patterns are measured from the direct luminescent *in situ* response to analyte binding.

Experiments previously performed by Xu and Song were reproduced and analyzed. Previous results indicated that residual template molecules remain attached to the binding sites even after soxhlet washing. All MIPs and NIP were washed 3 times in a 3mM acetonitrile solution of tetrabutylammonium (TBA) nitrate. To ensure that the synthesis of new polymer yielded similar results to previous tests, a comparison between newly synthesized and standard sample was measured as seen in Figure 1.1.

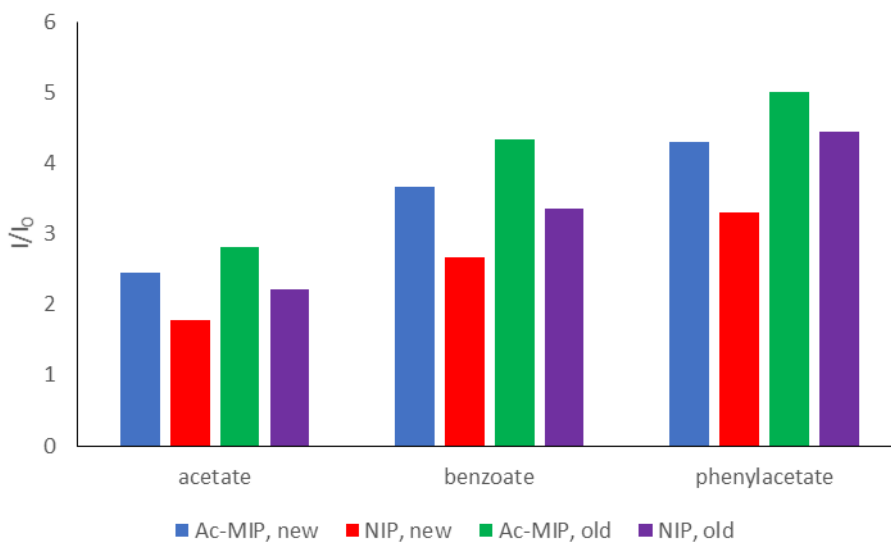


Figure 1.1. Comparison of old NIP (green) and Ac-MIP (purple) synthesized by Yang Xu and newly synthesized NIP (red) and AC-MIP (blue) against acetate, benzoate, and phenylacetate analytes. All samples underwent the nitrate washing technique prior to measuring the intensity. An excitation wavelength of 350 nm was used to obtain the emission at 616 nm for 0.01 g of polymer in 0.3 mL of acetonitrile.

Polymer was suspended in a 5:1 chloroform:acetonitrile solution and sonicated. Aliquots of 0.4 mL (0.01 g of polymer) were deposited into a quartz microtiter plate. After drying for several hours, 0.3 mL of acetonitrile were added to each sample and after 15 min, the luminescence was measured at an excitation of 350 nm.

To compare the luminescent intensities of the various MIPs, I/I_0 was used with I as the intensity of the polymer (P1-P5) emission with analyte solution and I_0 as the intensity

of the polymer in blank acetonitrile. While the older samples of NIP and Ac-MIP from Song and Xu produced consistently higher emission intensity than their newly synthesized counterparts, the general trend between the NIP and Ac-MIP's difference in intensity was preserved. This suggests that while the total emission intensity of polymers experiences batch to batch variations, the correlation between the different sensing elements remains constant. Because of this trend, large scale precursor synthesis was used so that the same batch of Eu-salen ligand was used for the NIP and three MIPs. A new batch of NIP and MIPs were synthesized using acetate, benzoate (Bz-MIP) and phenylacetate (Ph-MIP) templates.

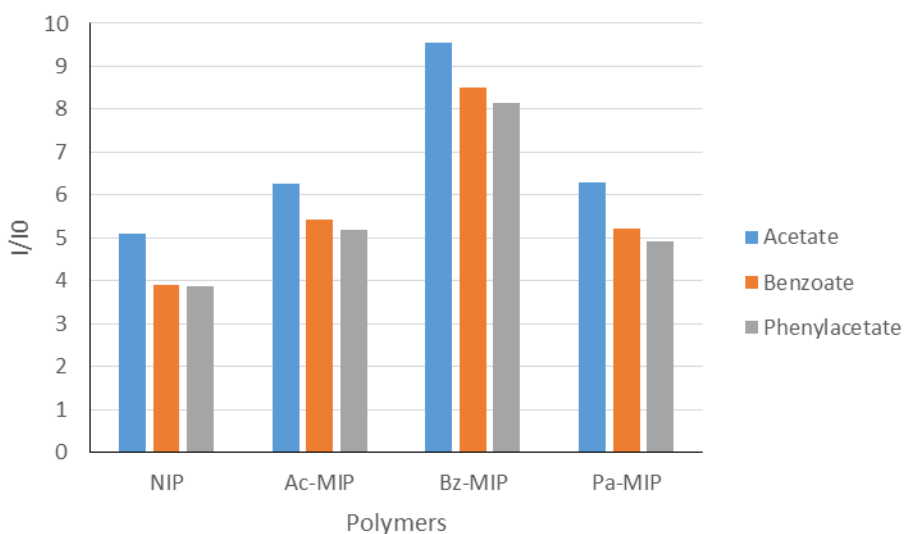


Figure 1.2. Average of five luminescent responses of NIP and three MIPs at 616 nm with the addition of 0.3 mL of 3 mM analytes TBA acetate, benzoate, and phenylacetate in acetonitrile. The polymers were excited at 350 nm.

However, while there is a clear difference between the total intensities, the trends between the analytes remain consistent. This would, for instance, make it difficult to distinguish the phenylacetate and benzoate with regards to the Ac-MIP and Pa-MIP. Full

spectra were taken of the emission profiles of the Eu-polymers in the presence of the analytes as well as several other anions seen in Figure 1.3.

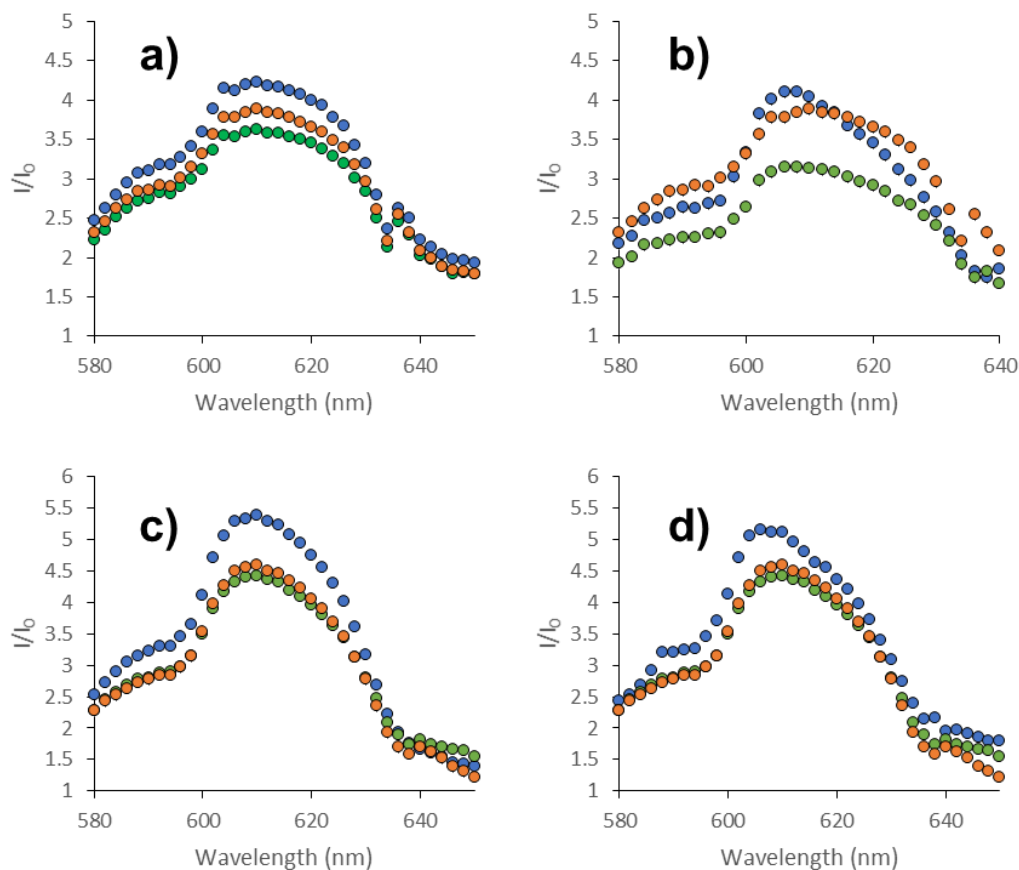


Figure 1.3. Average emission of NIP (a), Ac-MIP (b), Bz-MIP (c), Pa-MIP (d) over five measurements with the addition of 0.3 mL of 3 mM TBA acetate (blue), benzoate (green), and phenylacetate (orange) at when excited at 350 nm.

With the exception of the 610-640 nm range in Figure b for phenylacetate, the order and patterns of the analytes all remain consistent. However, often a great deal of variance is not discernable simply from visually comparing two spectra, so multivariable analysis was used to reduce the dimensionality of the data set and isolate any unique features of each response spectra and patterns.

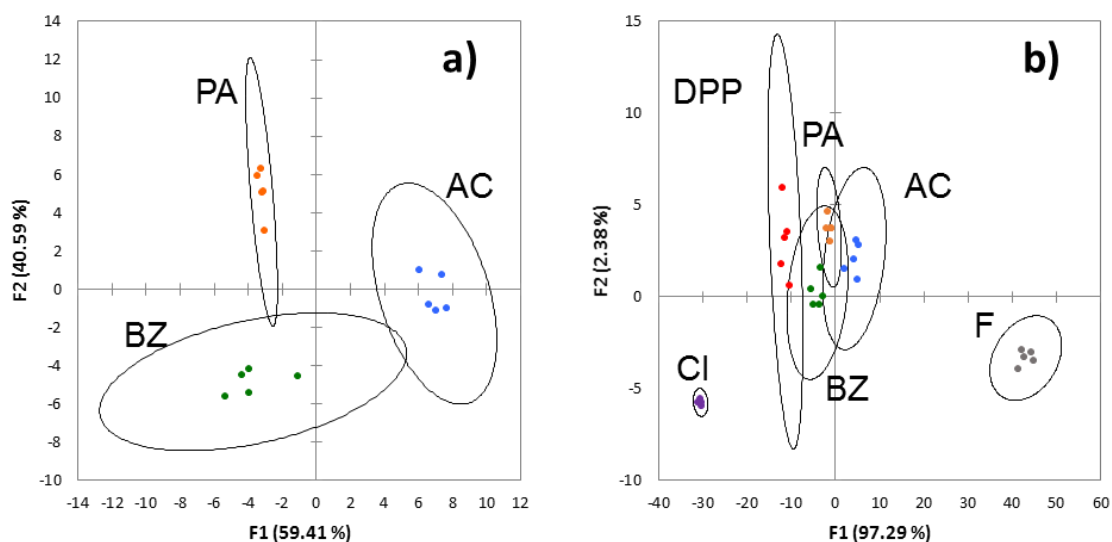


Figure 1.4. LDA analysis of sensor array with TBA-acetate (AC, Blue), benzoate (BZ, green), and phenylacetate (PA, orange) (a), and the analysis with the three template molecules and diphenyl phosphate (DPP, red), chloride (Cl, purple), and fluoride (F, gray) (b). The cross-validation of the analysis was 100% (a) and 97% (b).

While this process showed potential as an array, the molecular imprinting process did not appear to create significant affinity for the template molecule. Also, the inclusion of other analytes actually reduced the ability of the array to distinguish the carboxylates. While the lack of imprinting did not significantly impact the success of using this as an array, it does suggest that the imprinting process for this polymer system is unnecessary. The primary function of molecular imprinting was to create unique specificity for each sensing element.

The reason for the failure in imprinting is because the three templates only have a single functional group capable of creating specific recognition, the carboxylic acid. The direct binding site of the europium is the only site in the polymer matrix capable of interacting with the functional groups of the analytes. Because of the lack of non-covalent

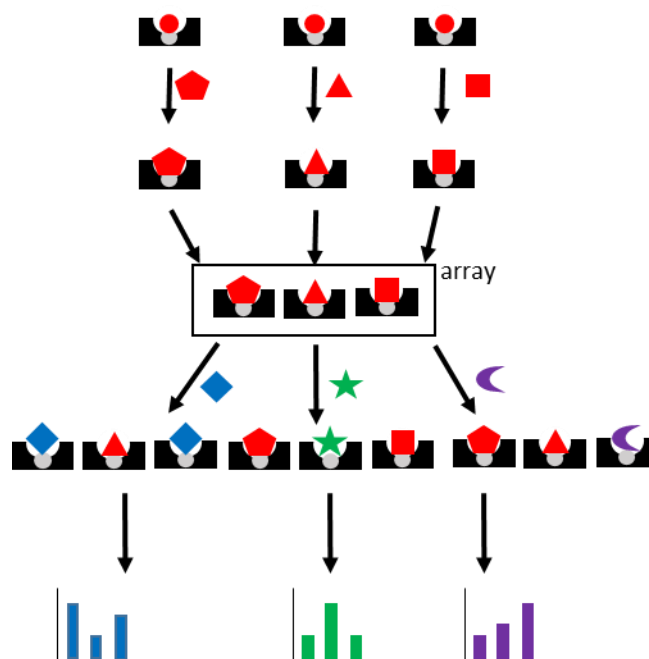
interaction sites on the analytes, contribution to creating specificity in the polymer matrix are nonexistent. Also, the design strongly followed Borovik's including the use of EGDMA as the crosslinking agent with no functional monomer such as methacrylic acid or methacrylamide. This system lacked both unique recognition sites on the template molecules and the functional monomer necessary to create effective imprinted polymers.

Thus, initial attempts to create molecularly imprinted polymers (MIPs) were unsuccessful. The most logical explanation is that the carboxylates chosen (acetate, benzoate, phenylacetate) were simply too similar with the only unique non-covalent binding site ($C=O$) in the same area. Therefore, the only imprinting factor is size dependence which plays a minor role with these similar sized analytes. As expected, acetate consistently showed a larger emission than benzoate and phenylacetate because of its smaller size and ability to access more binding sites. Further work with this system was not attempted because a size-exclusive sensor showed limited potential.

1.4 ANION DISPLACEMENT POLYMER SENSOR ARRAY

Analysis of the previous results showed that the intensity of the emissions and emission profile was highly dependent on whether the polymer was washed in a TBA nitrate solution or not. The template molecules were not completely removed during the soxhlet extraction of the imprinted polymers and this residual template was the cause of varied emissions in the imprinting studies. This was demonstrated by washing the polymers with TBA nitrate and observing that the "imprinted" polymers lost their unique emission profiles and coalesced into very similar signals. While this was problematic for the imprinting approach, it did suggest an alternate strategy to prepare polymers with different selectivities by washing the NIP in different anion solutions to afford different sensing

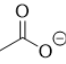
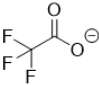
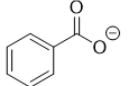
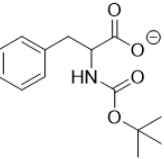
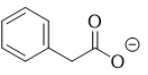
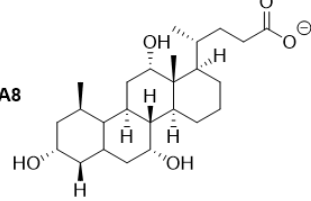
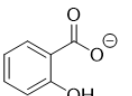
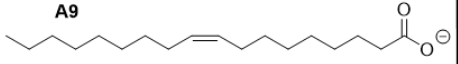
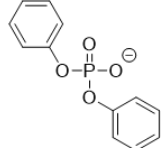
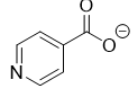
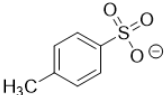
elements as seen in Scheme 1.2. This process was consistent with previously reported europium (III) host-guest displacement sensors.^{14, 15, 16}



Scheme 1.2. Representative scheme of the anion displacement array. The grey circles represent the europium binding site, the red shapes represent the anion host ligands, and the blue, green, and purple shapes represent analytes.

The host anions and carboxylate analytes are listed in Table 1.1 Host anions were chosen based on their diversity in size, shape, and basicity to maximize the signal variance. The carboxylate anions were chosen because of certain structural similarities. Analytes A1-A4 were chosen to test structurally similar molecules. They are also important food additives and preservatives. Analytes A5-A9 were added to test the size discrimination of the array. Specifically, analyte A6 was chosen due to the size and shape similarity with A2. Analyte A5 and A1 share similar sizes, but also have significantly different pKa's.

Table 1.1. Carboxylate analytes and host anions.

carboxylate analytes		host anions
A1 	A6 	P1 NO_3^-
A2 	A7 	P2 Cl^-
A3 	A8 	P3 SCN^-
A4 	A9 	P4 
A5 		P5 

The initial tests were performed to characterize the increase in luminescent emission with increasing concentrations of A1 as seen in Figure 1.5. The primary peak observed was the 618 nm $^5\text{D}_0$ to $^7\text{F}_2$ transition when the system was excited at 350 nm. The turn on luminescence of similar systems has been attributed to minor strains between the europium center and salen complex caused by different ligands binding at the open europium sites. A likely explanation is that the host anion (nitrate) is quenching or limiting the transfer of energy between the salen ligand and europium center when excited. Replacement of this ligand with A1 allows for greater transfer of energy and therefore an increase in emission from the system.

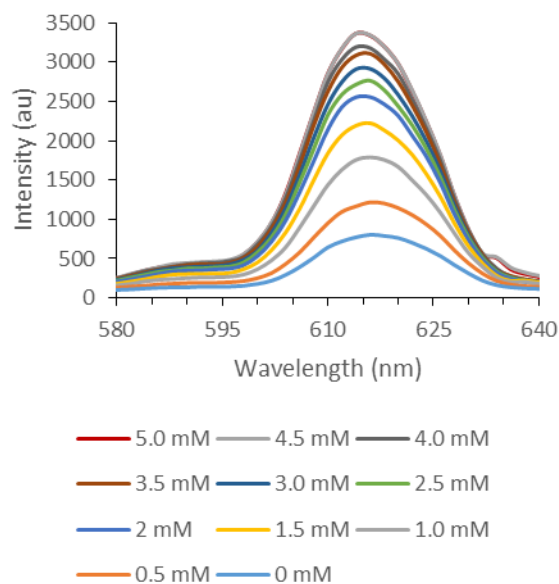


Figure 1.5. Change in fluorescent intensity of P1 with the addition of increasing concentrations of A1 when excited at 350 nm.

Further experimentation concluded that the optimal analyte concentration for further studies was 3 mM. The P1 polymer was titrated with A1, A2, and A3 of varying concentrations as seen in Figure 1.6. At this concentration, the response profile of the analytes showed a higher level of variation. This is also the lowest concentration at which the emission intensity for A2 and A3 is near the maximum difference.

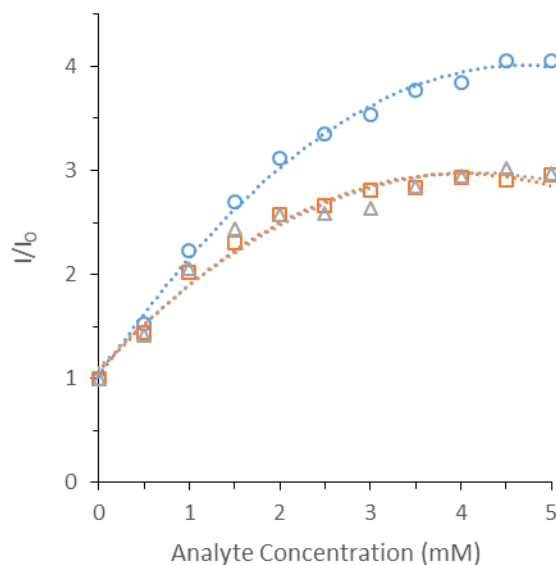


Figure 1.6. Titration curve of P1 luminescent response at 618 nm with the addition of varying concentrations of A1 (circles, blue), A2 (square, orange), A3 (triangle, gray) in acetonitrile (0.3 mL). P1 (0.01 g) was excited at 350 nm.

As was seen with the MIP array, A1 caused a larger increase in emission than A2 and A3 at the same concentration. The likely explanation for this is that the smaller A1 can access europium binding sites within the polymer that A2 and A3 are too large or sterically hindered to access. Further studies employed larger molecules to observe this trend.

The same process used to measure the MIP response was used to measure the response of the sensing elements (P1-P5) and were compiled into Figure 1.7.

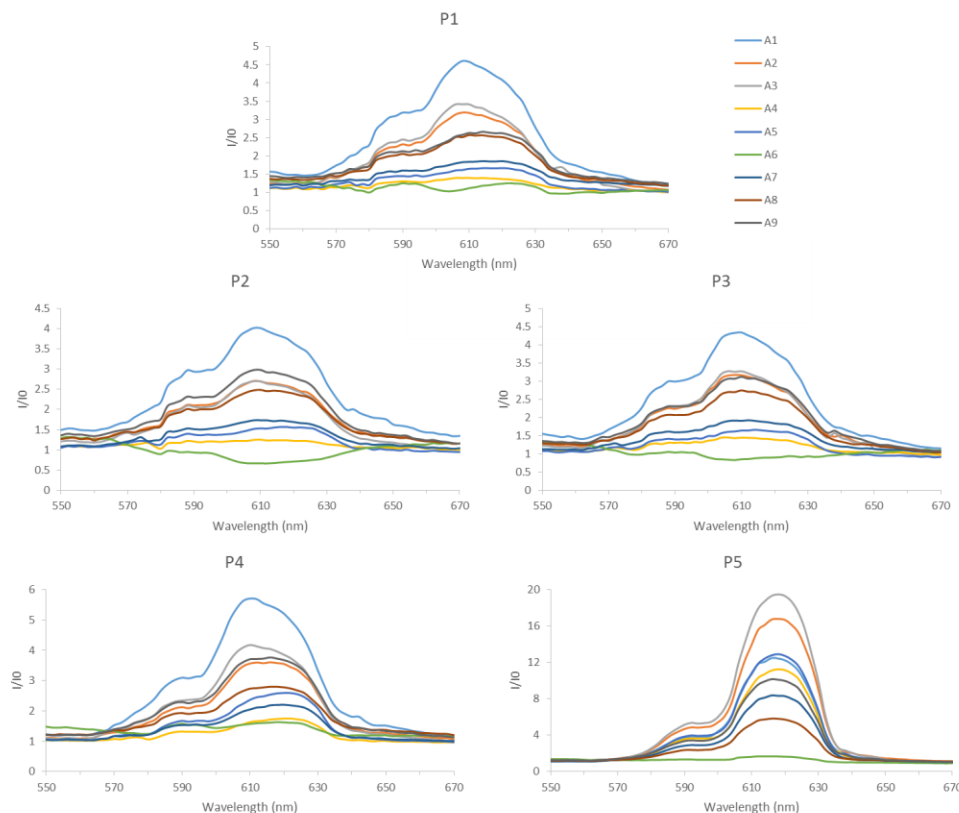


Figure 1.7. Emission spectra of the I/I_0 response of P1-P5 with the addition of A1-A9 excited at 350 nm.

In addition to differences in I/I_0 , the shapes of the emission spectra for P1-P3 retain similar characteristics. However, a significantly higher emission response was seen in P4 and P5 which showed a peak intensity more than double that of P4. Also of interest is the change in the order of the analytes in P5, namely that A1 no longer shows the greatest enhancement in emission. However, identification of key points of variation between are shown in Figure 1.8.

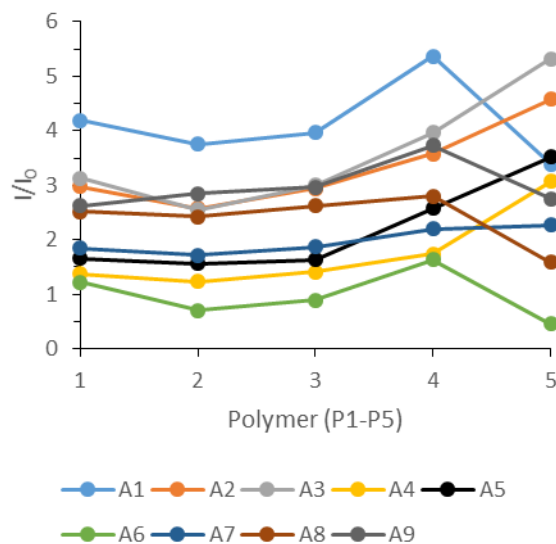


Figure 1.8. Luminescent response of the polymer array (P1-P5) against analytes (A1-A9) at 618 nm when excited at 350 nm. Each point is an average of 5 measurements, each measurement involved 0.01 g of dried polymer with the addition of 0.3 mL of 3 mM TBA-analyte solution in acetonitrile.

Despite minor shifts in intensity between P1-P3, most of the analytes appear to have a similar response along these sensor elements. Sensing element P4 sees several large spikes such as A1 and A5 while other analytes show a more minor increase like A7 and A8. Though subtle, differences like these can significantly increase the ability to distinguish analytes. However, the most interesting sensor, P5, shows a significant increase for some analytes and a significant decrease for others. Also, this is the only sensor where A1 does not have the strongest emission intensity. To characterize the visual differences seen in this figure, principle component analysis (PCA) was used. A software package of XL STAT 2016 was used to quantitatively assess the similarities and differences in the response patterns seen in Table 2.

Table 1.2. PCA contributions showing the variability of the individual sensor elements over all analytes and the entire spectrum (550-670 nm, all even wavelengths) when excited at 350 nm.

	<i>F1</i> %	<i>F2</i> %	<i>F3</i> %
total contributions	60.4	16.4	6.4
P1	24.5	6.4	3.6
P2	24.6	10.5	20.5
P3	24.1	9.6	8.8
P4	20.2	19.2	15.7
P5	6.6	54.5	49.1

The total contributions to the variance were equally spread between P1, P2, and P3 in the primary component (F1) with P4 and P5 contributing the least. However, P4 and P5 contribute the most to the secondary component.

The range between 578-588 nm was responsible for 13% of the total variance in the F1 component, and each wavelength (only even wavelengths) in that section had almost identical contributions (2.14-2.18%) over the 6 data points. Similar groupings were observed throughout F1, F2, and F3. To incorporate data from the entire spectrum, points were chosen in increments of 16 nm. The LDA plot is built from 584 nm, 600 nm, 616 nm, and 632 nm as seen in Figure 1.9.

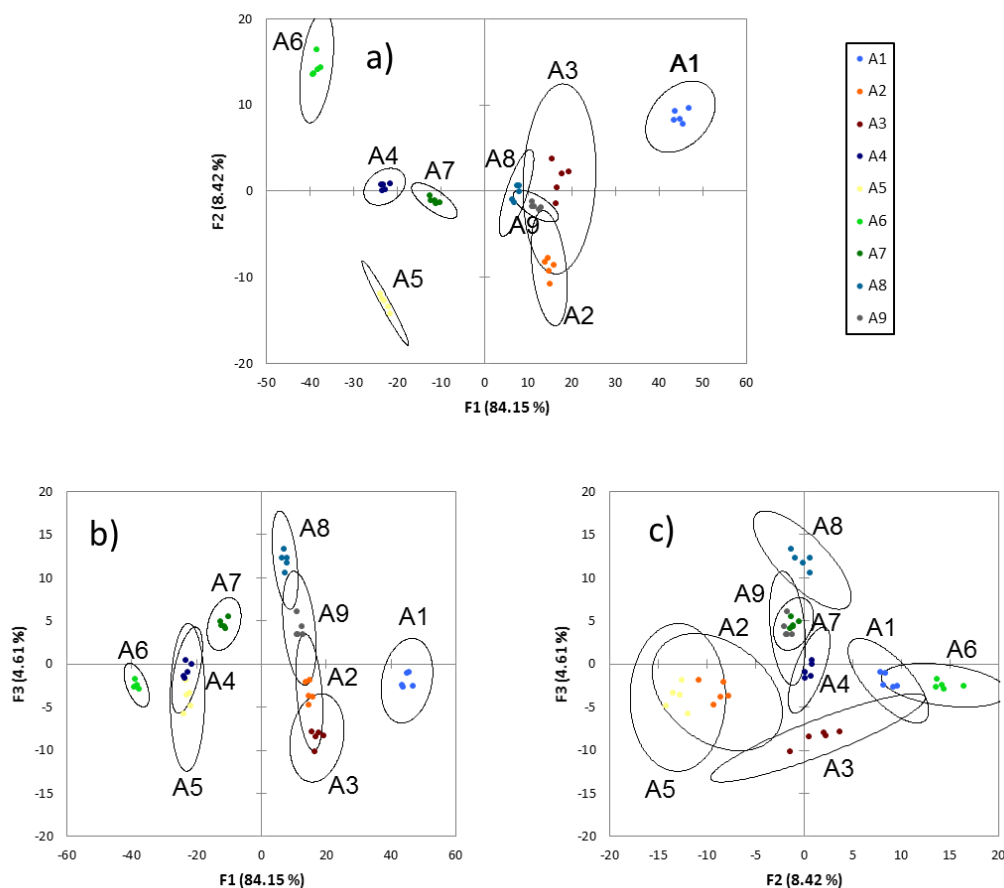


Figure 1.9. Two-dimensional LDA plots of the three most prominent linear discriminants. Centroids represent a confidence interval of 95%.

Analysis of the distances between the points for each pattern in the LDA plots did not show size and shape discrimination of the carboxylate of the analytes as a significant factor. For example, F1 did a poor job distinguishing A8 and A9, the two largest analytes, from A2 and A3. Also, A4 and A5 were distinctly separated from A2 and A3 despite having similar shapes. A more important parameter appears to be the relative basicity of the carboxylates. For example, A1 and A6 have both similar sizes and shapes but vastly different pKb's and were at opposite ends of the F1 scale. However, attempts to plot the discriminants (F1, F2, and F3) against the pKa's of the analytes showed no discernable

pattern. This suggests that the separation seen in this array is complex and based on several properties directly related to the individual analytes. The ability to discern these analytes based on their unique identities suggests that other analytes introduced into the system will also have a unique “fingerprint.”

To assess the classification accuracy of our luminescent polymer array, a jack-knife or “leave one out” cross validation was employed to describe the response quantitatively. This analysis treats a sample set of data like an unknown and performs the LDA analysis without this data set. After building the new library, the omitted data set is reintroduced and classified. This process is repeated for each sample pattern. Using this method resulted in 100% classification accuracy for this sensor array. This result demonstrates that the ligand exchange method of producing sensing elements can produce selective sensing elements. This is significant because of the simple method of preparation of the individual polymer elements of the array.

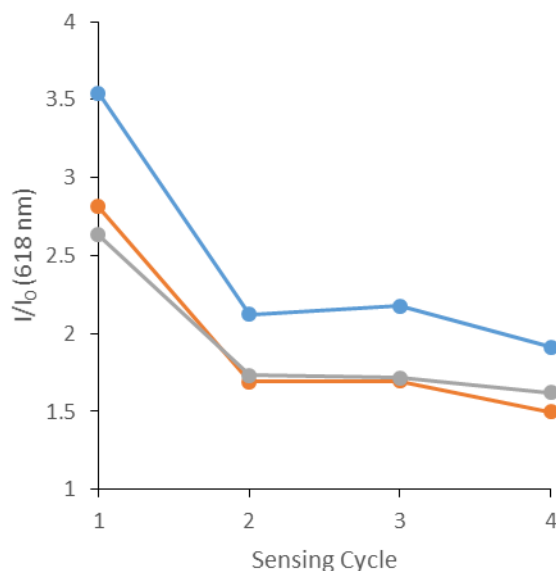


Figure 1.10. Change in the relative luminescent intensity at 618 nm with the reuse of nitrate washed polymer with the blue line as A1, orange line as A2, and gray line as A3. Polymers underwent a washing cycle with 10 mM TA-nitrate after each sensing cycle.

After the first use, the emission intensity significantly decreased, but remained more consistent with subsequent uses suggesting that the array may be reusable. One concern with the initial drop off in emission is that the primary component (F1) is directly related to the luminescent intensity as seen in Figure 1.11. Therefore, the primary contributor to the variance was significantly altered through multiple uses. However, the effect that this has on the system as a whole will likely be negligible. It has already been shown that P4 and P5 contribute the most significantly towards the second and third component which use less visually obvious patterns in the response to differentiate the analytes. These components are essential in separating certain analytes, and while a reduction in signal intensity will alter the fidelity in the F1 component, the distinct fingerprints should remain consistent.

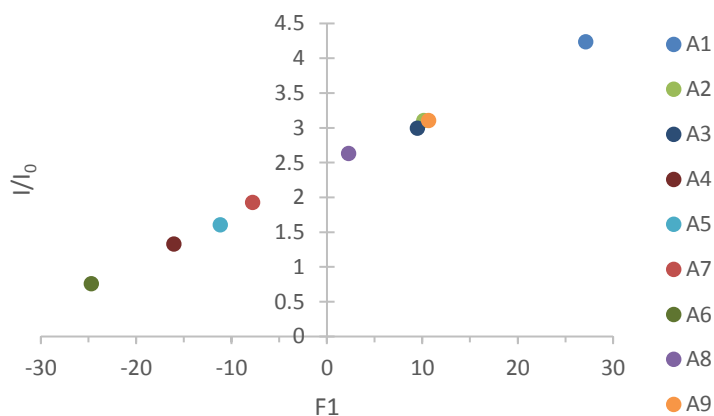


Figure 1.11 Correlation between F1 component and the change in intensity at 616 nm with an excitation at 350 nm.

An investigation into P4 and P5 was performed to determine why they contributed to F2 and F3 more significantly than P1-P3. Initial analysis of the data showed that both P4 and to a greater extent P5 had reduced I_0 emission along the entire spectrum (580-650

nm) than P1-P3. The turn on fluorescence of the polymer in the presence of carboxylate analytes has already been explained, and it is possible that both the diphenyl phosphate and *p*-toluene sulfonate anions negatively impact the transfer of energy between the salen ligand and europium center. Another theory is that there is a transfer of energy into diphenyl phosphate and *p*-toluene sulfonate that is lost through the resonance of the anion. The resonance quenching effect is a well-known phenomena, but regardless of the cause the lowered I_0 allows for an increased I/I_0 response for the system with the introduction of analytes and an extra level of variance during the competition of host and guest anions. To demonstrate the increased potential for variance, standard nitrate washed, hydrogen sulfonate washed, methane sulfonate washed, and *p*-toluene sulfonate washed polymer were compared in Figure 1.12.

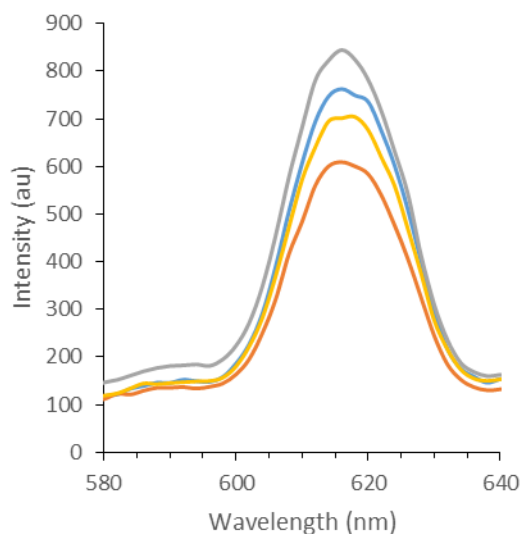


Figure 1.12. Luminescent intensity of polymer washed in various sulfonates. Standard nitrate washed (blue), hydrogen sulfonate (grey), methane sulfonate (yellow), *p*-toluene sulfonate (orange).

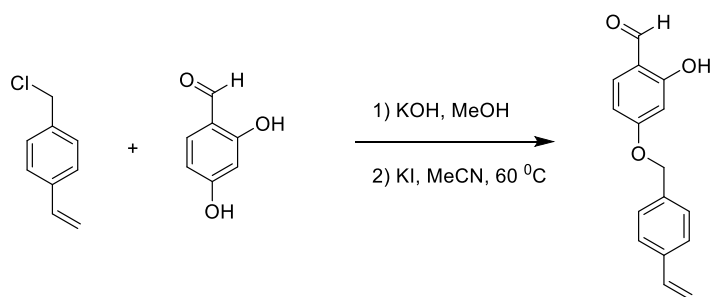
The most interesting aspect of this plot is that hydrogen sulfonate washed polymer exhibited a higher luminescent intensity than the standard nitrate washed polymer. In

addition, *p*-toluene sulfonate and methane sulfonate polymers both showed distinct emissions as well. The use of sulfonates as host anions in this array would be ideal for organophosphate sensing applications. Because phosphates and sulfonates have similar pKa's, their competition for the binding site should vary for any small conformational difference in hosts or analytes. Furthermore, using this method will incorporate resonance quenching affects as that are unique to the molecules.

In short, the effective use of a europium based luminescent polymer array based on anion ligand displacement has been demonstrated. The need to only synthesize a single batch of polymer tremendously simplifies the process of designing individual sensing elements. The washing technique to prepare the sensing elements is universal for TBA salts yielding a vast array of potential sensors. Specifically, it was determined that sulfonates acting as hosts affect the response signal in ways that the host anions of P1-P3 did not. An array consisting of sulfonates would likely provide even greater potential for the separation of analytes.

1.5 EXPERIMENTAL

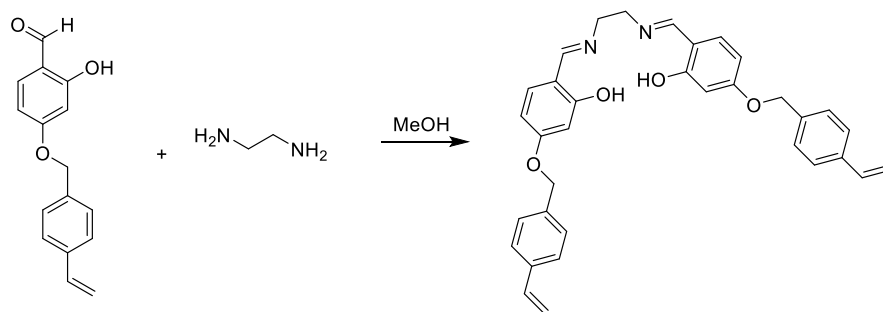
1.5.1 2-Hydroxy-4-(4-Vinylbenzyloxy)Benzaldehyde Synthesis



Scheme 1.3. Synthesis of 2-Hydroxy-4-(4-Vinylbenzyloxy)Benzaldehyde

To 30 mL of methanol, 2,4-dihydroxybenzaldehyde (10.4 g, 75 mmol) and potassium hydroxide (4.2 g, 75 mmol) were added and stirred for 30 minutes. Solvent was evaporated and residue was suspended in 50 mL of acetonitrile. A solution of vinylbenzyl chloride (9.16 g, 60 mmol) in acetonitrile was added. Potassium iodide (4.15 g, 25 mmol) was added and the mixture was heated at 50 °C for 10 hours. The reaction solution was filtered and the solution was collected. After evaporation of the solvent, 50 mL of water and 100 mL of ethyl acetate were added. The organic layer was collected and was washed with 3% potassium carbonate, water, and 5% citric acid each 3x. The solvent was removed in vacuo and the residue was recrystallized in ethyl acetate. The pure product is white rod-like crystal (38% yield). ^1H NMR (300 MHz, CDCl_3) δ : 9.72 (s, 1H), 7.40 (m, 5 H), 6.73 (dd, $J = 17.7$ Hz, $J = 10.8$ Hz, 1H), 6.61 (dd, $J = 8.7$ Hz, $J = 1.8$ Hz, 1 H), 6.51 (m, 1 H), 5.78 (d, $J = 17.7$ Hz, 1H), 5.28 (d, $J = 10.8$ Hz, 1H), 5.10 (s, 2 H).

1.5.2 Synthesis of Salen Ligand



Scheme 1.4. Synthesis of Salen.

The benzaldehyde (2.8 g, 11 mmol) was suspended in 50 mL of dry methanol and sonicated. The solution was put under nitrogen flow at 0 °C. Ethylenediamine (0.3 g, 5 mmol) was added dropwise in 3 parts over 30 min. The reaction mixture was taken off ice and stirred for 16 h. The precipitate was filtered and washed with ether. The yellow solid

was collected and dried (71% yield). ^1H NMR (300 MHz, CDCl_3) δ : 8.19 (s, 2H), 7.39 (m, 8H), 7.08 (m, $J = 8.4$ Hz, 2H), 6.71 (dd, $J = 17.7$ Hz, $J = 10.8$ Hz, 2 H), 6.45 (m, 4 H), 5.75 (d, $J = 17.7$ Hz, 2H), 5.25 (d, $J = 10.8$ Hz, 2H), 5.03 (s, 4 H), 3.85 (s, 4H).

1.5.3 Synthesis of Eu-salen Complex

Into 50 ml methanol, Salen (3.2 g, 6 mmol) and KOH (0.5g, 9 mmol) were added and stirred. A solution of europium nitrate hexahydrate (1.78 g, 4 mmol) in MeOH was added and stirred for 12 h at 40 °C. The precipitate was filtered and washed with methanol. (76% yield) yellow solid. UV-vis UV/Vis (DMF, λ_{max} , nm): 350 nm. Fluorescent emission (DMF, λ_{max} , nm): 614.

1.5.4 Polymerization of Eu-Salen Complex

$\text{Eu}_2(\text{salen})_3(\text{H}_2\text{O})_2$ (0.05 g) and EDGMA (0.95 mL, 5 mmol) was dissolved in 7 mL dichloroethane then heated at 80 °C. At this stage, templates for individual MIPs (TBA-acetate, benzoate, and phenylacetate) were added (0.312 mmol) or none were added for NIP. After complete dissolution of the materials, AIBN (0.016 g, 0.1 mmol) was added and the mixture was heated at 80 °C for 8 h. The resulting polymer was ground and sieved through a 150 micron sieve. Polymer was then washed with methanol for 12 h in a Soxhlet extractor, and then with a 1:4 methanol/acetonitrile mixture for another 12 h. Polymer was dried in vacuo to constant weight.

1.5.5 Tetrabutylammonium Carboxylates

To 50 mL methanol, carboxylic acid (4 mmol) and tetrabutylammonium hydroxide 30-hydrate (3.2 g, 4 mmol) were added and stirred for 6 hours. The solvent and water was removed through multiple high temperature rotovaps and the systematic addition of

toluene. A gray solid was collected. A gray solid was obtained with a 94% yield and verified with ^1H NMR.

1.5.6 Luminescent Studies

The desired polymer (0.16 g) was suspended in a 5:1 chloroform:acetonitrile solution (5.36/1.06 mL) using a sonicator, and 0.4 mL of solution (0.01 g) of polymer was deposited into a microtiter plate. The solvent was evaporated over the course of several hours and warmed on top of an oven. After cooling to room temperature, 0.3 mL of 3 mM analyte solution was added to the wells. After 15 minutes, fluorescence was measured over a range of 550-670 nm with an excitation at 350 nm.

1.6 REFERENCES

1. Duke, R.M.; Veale, E.B.; Pfeffer, F.M.; Kruger, P.E.; Gunnlaugsson, T. *Chem. Soc. Rev.* **2007**, *129*, 9856-9857.
2. Sakai, R. *Nature Polymer Journal.* **2016**, *48*, 59-65.
3. Haas, Y.; Stein, G.; *J. Phys. Chem.* **1971**, *76*, 3667-3677.
4. Mitchell-Koch, J.T.; Borovik, A.S. *Chem. Mater.* **2003**, *15*, 3490-3495.
5. Peczu, M.W.; Hamilton, A.D. *Chem. Rev.* **2000**, *100*, 2479-2494.
6. Kovala-Demertzi, D. *J. Organom. Chem.* **2006**, *691*, 1767-1774.
7. Akdeniz, A.; Mosca, L.; Minami, T.; Anzenbacher, P. *Chem. Commun.* **2015**, *51*, 5770-5773.
8. Davey, E.A.; Zuccherro, A.J.; Trapp, O.; Bunz, U.H.F. *J. Am. Chem. Soc.* **2011**, *133*, 7716-7718.
9. Han, J.; Bender, M.; Hahn, S.; Seehafer, K.; Bunz, U.H.F. *Chem. Eur. J.* **2016**, *22*, 3230.
10. Anzenbacher, P., Jr.; Lubal, P.; Bucek, P.; Palacios, M.A.; Kozelkova, M.E. *Chem. Soc. Rev.* **2010**, *39*, 3936-3953.
11. Johnson, K.J.; Rose-Pehrsson, S.L. *Annu. Rev. Anal. Chem.* **2015**, *8*, 287-310.

12. Askim, J.R.; Mahmoudi, M.; Suslick, K.S. *Chem. Soc. Rev.* **2012**, *42*, 8649.
13. Green, N.T.; Shimizu, K.D. *J. Am. Chem. Soc.* **2005**, *127*, 5695-5700.
14. Carr, R.; Bari, L.D.; Piano, S.L.; Parker, D.; Peacock, R.D.; and Sanderson, J.M. *Dalton Trans.* **2012**, *41*, 13154-13158.
15. Hammell, J.; Buttarazzi, L.; Huang, C.H.; Morrow, J.R. *Inorg. Chem.* **2011**, *50*, 4857-4867.
16. Shao, N.; Jin, J.; Wang, G.; Zhang, Y.; Yang, R.; Yuan, J. *Chem. Commun.* **2008**, 1127-1129.

CHAPTER 2

SOLVENT PROGRAMMABLE POLYMER

2.1 ABSTRACT

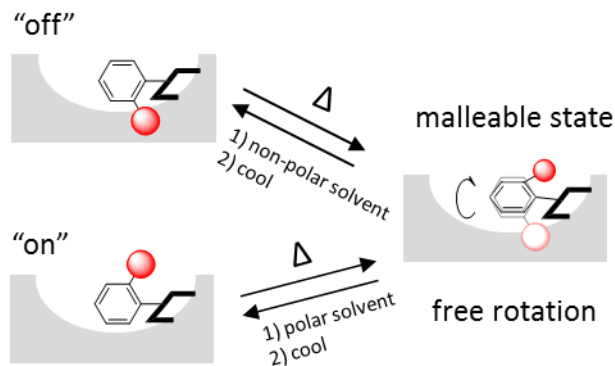
A solvent programmable polymer (SPP) based on the hindered bond rotation of carboxylic acid monomers was studied to determine the molecular memory mechanism and to create a greater variety of SPPs through free radical polymerization. The SPP was prepared by ring-opening metathesis polymerization (ROMP) which incorporated the atropisomeric functional monomer into a rigid crosslinked network. The orientation of the carboxylic acid groups was achieved by heating and then cooling in various solvents. These solvent-induced changes altered the recognition properties of the SPP and were retained at room temperature. The recognition properties were repeatedly erased and reprogrammed by heating in different solvents. The orientation of the carboxylate monomers was measured using ethyl adenine-9-acetate (EA9A), and the binding of EA9A increased with polar solvents and decreased with non-polar solvents. A new theory suggesting that dimerization between carboxylic acids is responsible for the decreased binding of EA9A is discussed. Also, attempts to create a monomer capable of free radical polymerization are documented.

2.2 INTRODUCTION

Materials with switchable properties have received much attention in recent years. A variety of stimulants can be used to force a transition from one molecular state to another, but retention of the second state typically relies on continued stimulation. A solvent programmable polymer capable of retaining programmed states is discussed herein.^{1,2,3}

The primary mechanism of the SPP relies on a hindered bond rotation that is kinetically restrained at room temperature. At higher temperatures, the SPPs are sterically unrestrained and can switch their recognition properties in response to interactions with solvent molecules. On cooling, the solvent-induced orientation of the monomers is retained through the reestablishment of restricted-rotation. Not only does the polymer display solvent memory, but it also provides a unique fingerprint based on the polarity of the solvent. Strong hydrogen bonding solvents such as water, methanol, and isopropanol increase the percentage of solvent accessible carboxylic groups and the binding capacity of the polymer. Conversely, less polar solvents such as cyclohexane, dioxane, and acetonitrile decreases the percentage of solvent accessible carboxylic acid groups and decreases the binding capacity of the polymer.

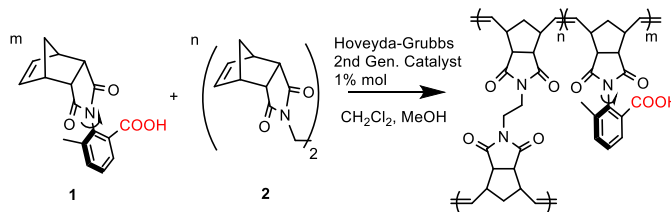
The initial hypothesis for the switching mechanism of the SPPs is shown in Scheme 1. The atropisomeric functional monomer with a carboxylic acid recognition group is shown against the polymer matrix. The carboxylic acid recognition group (red sphere) was positioned *ortho* to the C_{aryl}-N_{imide} bond so that its relative orientation and solvent accessibility would change with rotation as seen in the Scheme 2.1.^{4,5,6}



Scheme 2.1. Representative scheme of the initial theory of the SPP's rotational mechanism when heated and cooled in polar and non-polar solvents.

2.3 "TURN-OFF" DIMERIZATION

The initial mechanistic hypothesis was based on the assumption that the polymer matrix was rigid enough to shield the solvent accessibility of the carboxylic acid monomers. It was believed that this highly crosslinked morphology would result from the ROMP polymerization of the monomer and crosslinker seen in Scheme 2.2.

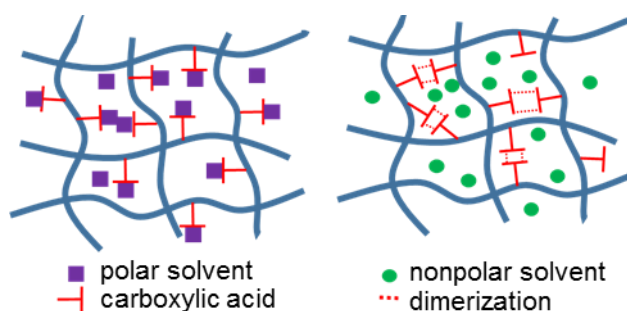


Scheme 2.2. Preparation of the SPP with the functional monomer (1) and the crosslinker (2).

However, previous experimental results collected by Zhang and He do not show consistent results with this theory. The characterization of the ROMP SPP was more consistent with a gel morphology. This conclusion was based on the following observations. First, results from Yinyan's experiments show a higher level of polymer swelling percentages than expected for rigid polymers. Dried polymer particles were combined with various solvents and swelling percentages of 50%, 42%, and 30% were

observed for acetonitrile, cyclohexane, and water respectively. Second, an acid-base titration performed on the SPP by Yagang showed that the accessibility of the carboxylates did not change based on which solvent the SPP was heated and cooled in. The theoretical number of carboxylic acids in the SPP (0.578 mmol/g) was based on the ratios of monomer **1** and crosslinker **2** used in the ROMP. Approximately 57% of these sites were susceptible to deprotonated. SPP heated and cooled in cyclohexane and SPP heated and cooled in water were both found to vary less than 1%.

The combination of swelling properties and accessible sites suggests that the SPP contained well solvated polymer chains that retain accessible functional sites regardless of the rotamer. The polymer system is therefore more consistent with a gel morphology than the highly crosslinked system initially described. In order to incorporate these two studies with the results seen in the EA9A binding studies, a new mechanism was proposed. The recognition properties of the carboxylic acid sites are dictated by the formation of dimers as seen in Scheme 2.3.



Scheme 2.3. Representation of the new theory suggesting that the “off” state of the SPP is caused by the dimerization of carboxylic acid moieties.

When heated in a polar solvent, the solvated carboxylic acids rotate to maximize their interactions with the solvent molecules. After cooling, the carboxylic acids become fixed in these solvent and guest accessible orientations. When heated in a nonpolar solvent,

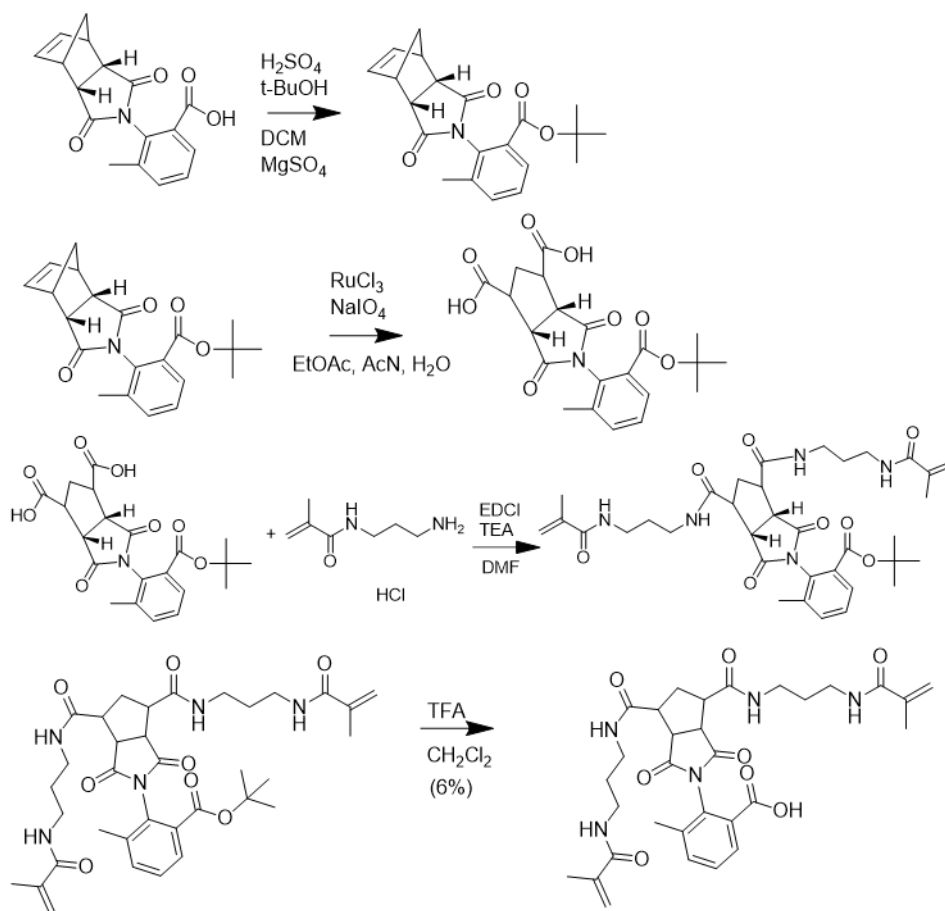
the carboxylic acids rotate to avoid the non-polar solvent by forming strong hydrogen bonded dimers. This dimerized conformation reduces the accessibility of the carboxylic acids. Strong bases such as the NaOH used in the titration experiment are capable of disrupting the dimer and deprotonating the acids, but weakly basic guests such as EA9A do not disrupt the dimer. This allows for the decreased binding percentages of EA9A after heating in non-polar solvent while also explaining the similar quantity of accessible sites for NaOH.

2.4 FREE RADICAL SYNTHESIS

The process of ROMP reactions relies heavily on ring strain to create a polymer network. This constraint limits the ability to study a variety of functional monomers that might result in SPPs. Free radical polymerization can occur with acrylate, acrylamide, and styrene groups which can be easily attached to existing structures. The goal of this project was to incorporate functional groups onto the monomer that would participate in free radical polymerization.

The primary strategy for this synthesis was to open the sp² bond in the norbornene section of the molecule and attach acrylate, acrylamide, or vinyl functional groups that could participate in free radical polymerization. The functional monomer used in the ROMP polymerization exists as a single rotamer and this constraint is due to the steric hindrance caused by the sp² bond. Initial trials protected the carboxylic acid recognition group as a methyl ester, but the deprotection was found to react with the imide portion of the molecule. Instead, a tert-butyl ester group was used. Sulfuric acid and MgSO₄ were mixed prior to the addition of the monomer and t-butanol, and the reaction was driven with the absorption of water byproduct by excess MgSO₄. Next, a combination of RuCl₃ and NaIO₄ in a 2:2:3 ratio of ethyl acetate, acetonitrile, and water was used to oxidize the

norbornene sp² bond into two carboxylic acids. The biphasic solution was vigorously stirred several hours and a dicarboxylic acid was obtained after filtration and base to acid extraction. The acrylamide was attached using EDCHCl in dry DCM. And finally, the deprotection of the original carboxylic acid was performed with H₃PO₄ in acetonitrile seen in Scheme 2.4.

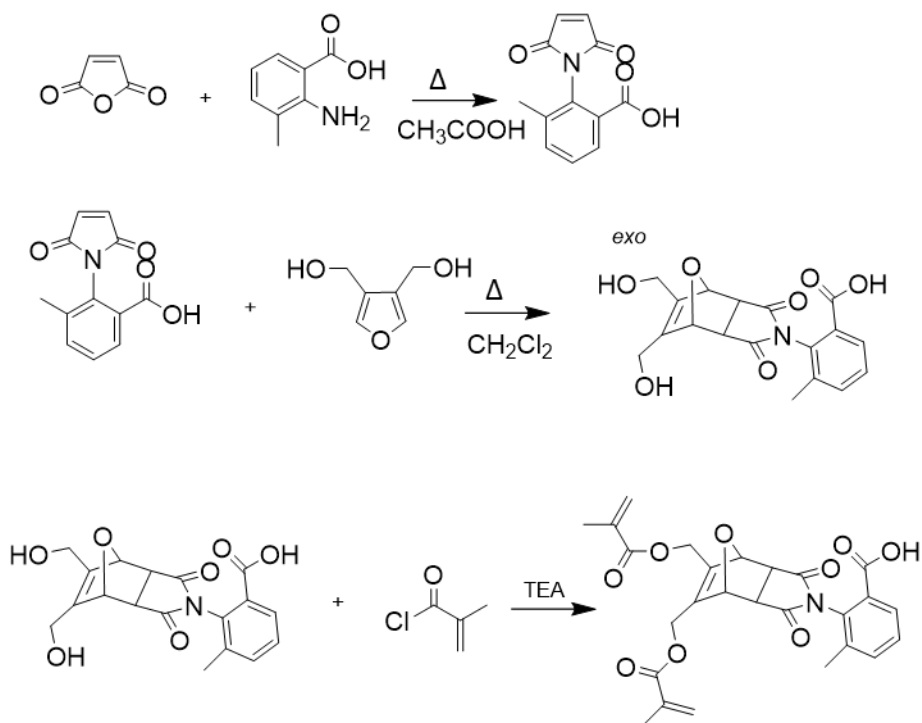


Scheme 2.4. Synthesis route for the incorporation of acrylate groups onto the functional monomer.

Identification of the dicarboxylic acid proved to be challenging based on the NMR. All peaks were identified and characterized except for the acid peak expected to appear above 10 ppm. TLC and bromocrescol green stain supported the inclusion of an acid group in the structure. A coupling reaction using EDCHCl in MeOH was performed on a small

amount of purified material to verify the presence of 2 carboxylic acid groups. Integration of the methyl ester peak in $^1\text{H NMR}$ showed the incorporation of two methyl esters into the molecule demonstrating the presence of the acid groups in the previous molecule.

The cause of the low deprotection reaction yield was not identified, but it is possible that the acid used catalyzed a polymerization reaction. Subsequent attempts to perform this synthesis demonstrated that the t-butyl protection reaction was unreliable. In addition, use of an acrylamide instead of an acrylate was based on the notion that the deprotection of a ester protecting group could cleave an acrylate group. To resolve these problems a new synthesis is proposed.



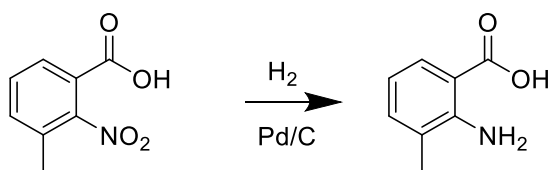
Scheme 2.5. Proposed synthetic route to incorporate acrylate functional groups onto a potential monomer for a SPP polymer.

The proposed mechanism relies on the Diels Alder reaction between a furan and imide resulting in an *exo* product.^{7, 8} Typically *endo* products are favored in Diels Alder

reactions which is why this conformation has been used so far in the design of the SPP. However, Diels Alder reactions that include furans have been shown to yield the more thermodynamically stable *exo* product in place of the more kinetically stable *endo* product. The presented procedure should resolve the steric hindrance cause by the endo norborene monomer used previously and does not rely on the protection of the carboxylic acid recognition site.

2.5 EXPERIMENTAL

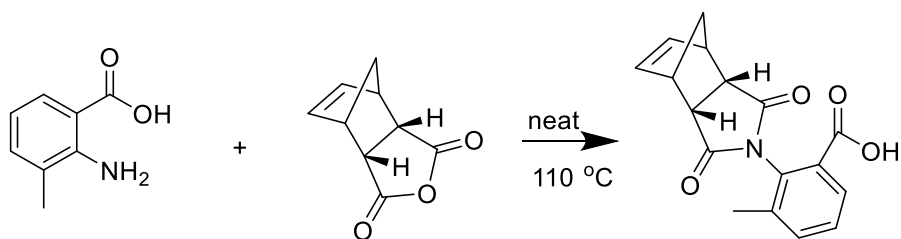
2.5.1 2-Amino-3-Methylbenzoic Acid Synthesis



Scheme 2.6. 2-amino-3-methylbenzoic acid synthesis.

3-methyl-2-nitrobenzoic acid (5 g, 28 mmol) was hydrogenated overnight with 10% by weight palladium on carbon in ethanol. Solution was filtered and dried under vacuum to produce a reddish-brown powder for a 92% yield. ^1H NMR (Acetone- d_6 , 300 MHz) δ ppm: 8.00 (s, 1H) 7.73 (d, $J = 7.73$ Hz, 1H), 7.17 (d, $J = 7.17$ Hz, 1H), 6.49 ($J = 6.49$, 1H), 2.16 (s, 3H).

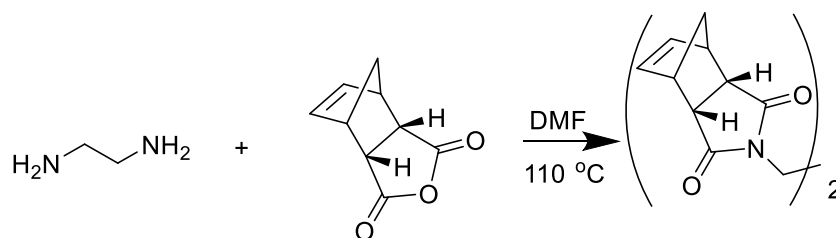
2.5.2 ROMP Monomer Synthesis



Scheme 2.7. Synthesis for functional ROMP monomer.

2-amino-3-methylbenzoic acid (1.25 g, 8 mmol) and cis-5-norbornene-endo-2,3-dicarboxylic anhydride (1.5 g, 9 mmol) were combined and dissolved in THF. The solvent was removed by vacuum, and the remaining solid was put under vacuum and heated overnight at 110 °C for a 94% yield. Product was a brown solid. ¹H NMR (Acetone-d₆, 300 MHz) δ ppm: 7.95 (d, *J* = 7.8 Hz, 1H), 7.57 (d, *J* = 7.8 Hz, 1H), 7.44 (dd, *J* = 7.5 Hz, 1H), 6.32 (dd, *J* = 2.1 Hz, *J* = 1.8 Hz, 2H), 3.50-3.52 (m, 2H), 3.37-3.39 (m, 2H), 2.12 (s, 3H), 1.73 (dd, *J* = 1.5 Hz, 2H).

2.5.3 Crosslinker Synthesis



Scheme 2.8. Synthesis for ROMP crosslinker.

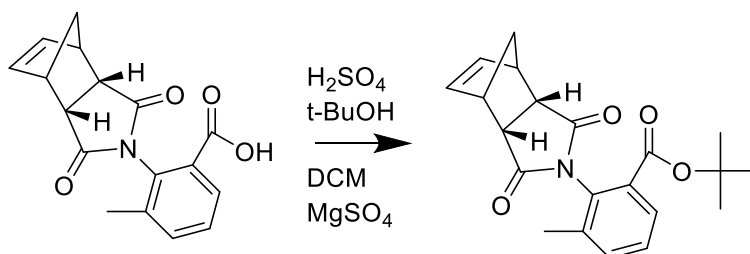
Norbornene-endo-dicarboxylic anhydride (0.743 g, 4 mmol) and ethylene diamine (0.14 mL, 0.002 mol) were dissolved in DMF and refluxed at 110 °C for 24 hours. Addition of ice-cold water to the mixture crashed out a precipitate which was filtered and washed with water. White solid was dried in vacuo, 73% yield. ¹H NMR (CDCl₃ 300 MHz) δ ppm: 6.03 (dd, *J* = 2.1 Hz, *J* = 1.8 Hz, 4H), 3.45 (s, 4H), 3.32 (m, 4H), 3.22 (m, 4H), 1.71 (d, *J* = 8.7 Hz, 2H), 1.51 (d, *J* = 8.6 Hz, 2H).

2.5.4 ROMP Polymerization

80/20 mole % mixture of crosslinker (0.75 g, 2.2 mmol) to functional monomer (0.16 g, 0.55 mmol) was dissolved in 6 mL of CH₂Cl₂ and 3 mL of MeOH. Hoveyda-

Grubbs Gen. 2 catalyst (0.016 g, 26 μ mol) was added and the mixture was shaken for 20 min. Reaction proceeded at room temp for 10 hours, and was heated at 60 $^{\circ}$ C for 4 hours. The polymer was dried, ground, and washed in a soxhlet extractor for 24 hours with methanol and then for another 24 hours with 4:1 methanol/acetonitrile.

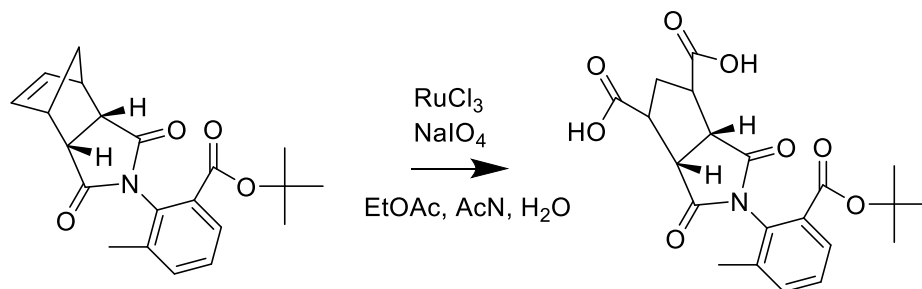
2.5.5 T-Butyl Protecting Group Incorporation



Scheme 2.9. Synthesis of t-butyl protected monomer.

In 40 mL of DCM, MgSO_4 (4.81 g, 40 mmol) was combined with H_2SO_4 (0.55 mL, 10 mmol) and stirred vigorously for 15 min. The carboxylic acid (2.97 g, 10 mmol) and $t\text{-BuOH}$ (4.78 mL, 50 mmol) were added, and the reaction was stirred overnight. A solution of 70 mL saturated sodium bicarbonate solution was added and stirred until MgSO_4 was consumed. Organic phase was washed with brine, dried with MgSO_4 , and recrystallized in MeOH to obtain a white/brown crystals at 35% yield. ^1H NMR (Acetone- d_6 , 300 MHz) δ ppm: 7.95 (d, $J = 7.8$ Hz, 1H), 7.57 (d, $J = 7.8$ Hz, 1H), 7.44 (dd, $J = 7.5$ Hz, 1H), 6.32 (dd, $J = 2.1$ Hz, $J = 1.8$ Hz, 2H), 3.50-3.52 (m, 2H), 3.37-3.39 (m, 2H), 2.12 (s, 3H), 1.73 (dd, $J = 1.5$ Hz, 2H).

2.5.6 Oxidation of the Norbornene C=C

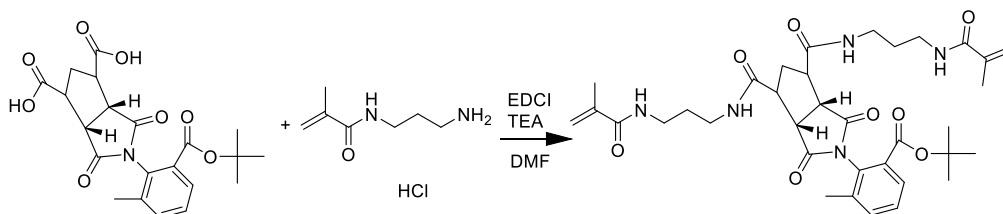


Scheme 2.10. Oxidation of norbornene C=C bond.

T-butyl protected imide (0.179 g, 0.5 mmol) was combined with 2 mL of ethyl acetate and 2 mL of acetonitrile at 0 °C. RuCl₃ (0.0023 g, 10 μmol) was added and stirred for 10 min while 3 ml of water was combined with NaIO₄ (0.432 g, 2 mmol). The aqueous solution was added to the solvent solution dropwise. Biphasic solution was taken off ice and stirred vigorously for 6 hrs. Solution was filtered and combined with 0.25 M aqueous NaOH solution. The aqueous solution was extracted and acidified to a pH 1 with HCl. Ethyl acetate was mixed with solution and solvent phase was extracted. Solvent was removed in vacuo and dicarboxylic acid was obtained as a white powder at an 83% yield.

¹H NMR (MeOH-d₄, 300 MHz) δ ppm: 7.89 (d, *J* = 7.81 Hz, 2H), 7.53 (d, *J* = 7.54 Hz, 1H), 7.40 (t, *J* = 7.41 Hz, 2H), 3.75 (dd, *J* = 3.73 Hz, 2H), 3.23 (m Hz, 2H), 2.33 (dd, *J* = 2.36 Hz, 1H), 2.27 (s, 3), 1.99 (s, 1H), 1.50 (s, 9H).

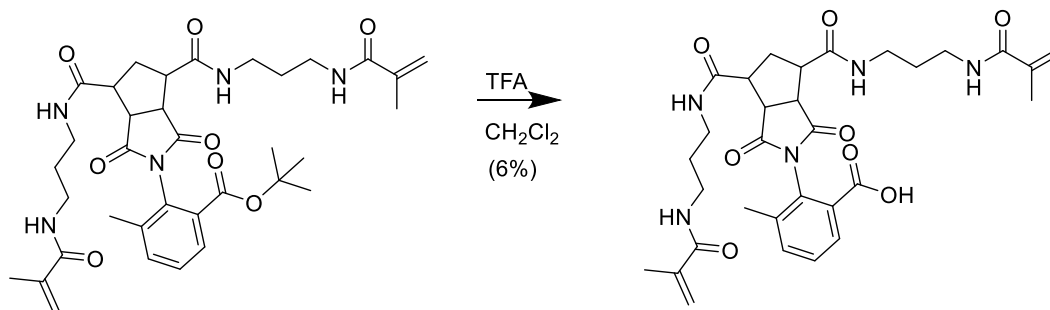
2.5.7 Amide Coupling



Scheme 2.11. Acrylamide coupling reaction.

N-(3-aminopropyl) methacrylamide HCl (0.05 g, 0.28mmol) was suspended in dry CH_2Cl_2 and cooled to 0 °C. Triethylamine (40 μL , 0.28mmol) was combined with dry CH_2Cl_2 and added dropwise to solution. Dicarboxylic acid (0.05 g, 0.12mmol) and EDCHCl (0.1 g, 0.52 mmol) were added and the solution was removed from ice and stirred for 12 h. Solvent layer was washed with water 3x and dried in vacuo. Resulting product was a white powder with 89% yield. ^1H NMR (MeOH- d_4 , 300 MHz) δ ppm: 8.16 (t, $J=8.16$ Hz, 2H), 7.89 (t, $J=7.88$ Hz, 2H), 7.78 (d, $J=7.81$ Hz, 1H), 7.54 (d, $J=7.54$ Hz, 2H), 7.39 (t, $J=7.48$ Hz, 2H), 5.67, 5.30 (d, $J=5.30$ Hz, 4H), 3.64 (dd, $J=3.64$ Hz, 2H), 3.36 (m, 4H), 3.20 (m, 2H), 3.12 (m, 4H), 2.55 (dd, $J=2.60$ Hz, 1H), 2.40 (s, 3), 1.99 (m, 1H), 1.87 (s, 6H), 1.75 (m, 4H), 1.50 (s, 9H).

2.5.8 T-Butyl Deprotection



Scheme 2.12. Deprotection of meth acrylamide functional monomer.

T-butyl protected monomer (0.1 g, 0.15 mmol) was dissolved in 2 mL of CH₂Cl₂ and 1 mL of trifluoroacetic acid was added dropwise. Solution was stirred for 3 h and water was added. Solvent layer was removed and dried in vacuo. Yield of 6% ¹H NMR (MeOH-d₄, 300 MHz) δ ppm: 8.16 (t, J = 8.16 Hz, 2H), 7.89 (t, J = 7.88 Hz, 2H), 7.78 (d, J = 7.81 Hz, 1H), 7.54 (d, J = 7.54 Hz, 2H), 7.39 (t, J = 7.48 Hz, 2H), 5.67, 5.30 (d, J = 5.30 Hz, 4H), 3.64 (dd, J = 3.64 Hz, 2H), 3.36 (m, 4H), 3.20 (m, 2H), 3.12 (m, 4H), 2.55 (dd, J = 2.60 Hz, 1H), 2.40 (s, 3), 1.99 (m, 1H), 1.87 (s, 6H), 1.75 (m, 4H).

2.5.9 Binding Studies

Polymer was heated and stirred in a sealed container of the desired solvent at 80 °C for 24 h. The mixture was cooled and the polymer was removed and washed with acetonitrile 5x. Polymer was then dried in vacuo.

Polymer (60 mg) was added to 2.5 mL of 0.1 mM EA9A and shaken for 2 hours. The polymer was separated from the solution, and UV-vis at 257 nm was used to quantify the difference between the starting EA9A solution and the solution exposed to the polymer.

2.5.10 Swelling Studies.

Ground polymer (160 mg) was placed in 5 mm NMR tubes. Excess water, hexane, or acetonitrile was added and heated at 83 °C for 26 h. The volume of swelling was determined by measuring the heights of the dry polymers versus the solvent heated polymers.

2.6 REFERENCES

1. Degenhardt, C., III; Shortell, D. B.; Adams, R. D.; Shimizu, K. D. *J. Chem. Soc., Chem. Commun.* **2000**, 929-930.
2. Chong, Y. S.; Shimizu, K. D. *Synthesis*. **2002**, 9, 1239-1244.
3. Rasberry, R. D.; Shimizu, K. D. *Org. Biomol. Chem.* **2009**, 7, 3899-3905.
4. Choi, D. S.; Chong, Y. S.; Whitehead, D.; Shimizu, K. D. *Org. Lett.* **2001**, 3, 3757-3760.
5. Lavin, J. M.; Shimizu, K. D. *Chem. Commun.* **2007**, 228-230.
6. Degenhardt, C. F.; Lavin, J. M.; Smith, M. D.; Shimizu, K. D. *Org. Lett.* **2005**, 7, 4079-4081.
7. Lee, M.W.; Herndon, W.C. *J. Org. Chem.* **1978**, 43, 518.
8. McElhanon, J.R.; Wheeler, D.R. *Org. Lett.* **2001**, 3, 2681-2683.